JOURNAL OF CATALYSIS **161,** 641–650 (1996)
ARTICLE NO. 0226

A Proposed Mechanism for Silica Supported Chromium HDPE Catalyst Activation

Steve M. Augustine and Jonathan P. Blitz

Allen Research Center, Quantum Chemical Company, Cincinnati, Ohio 45249; and Department of Chemistry, Eastern Illinois University, Charleston, Illinois 61920

Received August 28, 1995; revised March 7, 1996; accepted March 18, 1996

The decomposition of $Cr_3(C_2H_3O_2)_7(OH)_2/SiO_2$ in oxidizing, inert, and reducing environments was studied using isothermal kinetics, temperature-programmed reaction (TPRxn), and variable-temperature diffuse-reflectance infrared spectroscopy (VT-DRIFTS). Based upon these results a mechanism is proposed for the activation of silica-supported basic chromium acetate. The decompositions in N_2 and CO/N_2 mixtures appear very similar. The activation energies are within experimental error, and both exhibit second-order rate dependencies with respect to the surface acetate species. TPRxn results show that the Cr compound influences support dehydroxylation, but VT-DRIFT spectra show no evidence of Cr bonding to the SiO_2 surface. When CO is present, silica dehydroxylation appears to proceed via a water–gas shift type of reaction producing CO_2 and H_2 rather than H_2O. In oxygen, Cr compound decomposition occurs at temperatures 90°C lower than in inert or reducing environments. The reaction orders are 1/2 for oxygen and 1 for the surface acetate species. The activation energy is comparable to that calculated for the other two media. VT-DRIFT spectra show that oxygen induces a greater degree of hydroxyl removal and formation of Cr–O/Cr=O bonds concurrent with and subsequent to recorded decomposition temperatures. In this way they support TPRxn findings and suggest Si–O–Cr bond formation. It appears that the rate-limiting step in the activation mechanism is removal of the acetate methyl group. In oxygen this involves dissociative activation of oxygen on the Cr center and subsequent combustion. In the other environments migration is necessary to allow hydrogen transfer between two acetate groups to form methane and leave behind a hydrocarbon fragment. This explains the different temperatures of decomposition in the various media and the second-order rate dependence upon acetate in N_2 and CO/N_2. The lack of apparent Cr–SiO_2 bond formation in nonoxidizing environments allows surface migration of Cr compounds which makes this mechanism feasible.

INTRODUCTION

Silica-supported chromium catalysts have attracted much attention over the years primarily for two reasons. The first is due to their commercial impact in the production of billions of pounds of high-density polyethylene (HDPE) annually (1). The second is related to the technical debate surrounding the nature of the catalytically active site (2). Each of these issues is extremely important, and deciphering the latter is particularly challenging. However, the high level of interest directed toward these areas has limited the study of more elementary issues of catalyst preparation.

There is general agreement that Cr/SiO_2 HDPE catalyst performance is very sensitive to support hydroxyl population (2–4). The activity passes through a maximum with increasing dehydroxylation. Polymer melt index and molecular weight are also affected (5). Several factors influence the degree of SiO_2 dehydroxylation and, thus, catalyst performance. One among these is metal loading. Since Cr and surface silanols bond during oxygen activation via a condensation mechanism, increasing Cr content increases dehydroxylation (6). Another factor is treatment temperature. Higher temperatures effect a greater degree of hydroxyl removal, which favors catalyst activity until a threshold is reached. Past the threshold, activity declines due to sintering (5). A third factor involves the chemical medium in which the dehydroxylation is done. Activation in CO appears to be particularly effective for removing surface hydroxyl groups. It has been proposed that this is due to a mechanism analogous to the water–gas shift reaction (5, 7).

The purpose of this study is to determine the kinetics of the high-temperature activation step. We have studied basic chromium acetate ($Cr_3(C_2H_3O_2)_7(OH)_2$) decomposition with isothermal kinetics, temperature-programmed reaction (TPRxn) methods, and variable-temperature diffuse-reflectance infrared spectroscopy (VT-DRIFTS). The acetate ligands are used to follow the decomposition of the Cr compound both spectroscopically and via the evolution of gaseous products. The decompositions are done in reducing (CO in N_2 mixtures), inert (N_2 only), and oxidizing (O_2 in N_2 mixtures) atmospheres to determine the effect of the gas stream reagent.

0021-9517/96 $18.00

METHODS

Catalyst and Reagents

The catalyst precursor was basic chromium acetate supported on SiO_2. The sample was made by contacting silica with a surface area of ca. 300 m^2/g (PQ Corporation, used as received) with a methanolic (Fischer Scientific, 99.9% purity) solution of $Cr_2(C_2H_3O_2)_7(OH)_2$ (Strem Chemicals). Methanol was removed at 50°C using a rotary evaporator under mild vacuum. The final catalyst had a Cr content of 0.91 wt% as determined by ICP.

All gases (O_2, N_2, CO, >99.9%, Matheson) were dried with a 5 Å molecular sieve prior to use. Gas mixtures of 3–20% CO in N_2 and 5–21% O_2 in N_2 were made by mixing the respective gases with calibrated mass flow controllers.

Procedures

Temperature-programmed experiments were conducted on 100 mg samples of catalyst using a plug flow microreactor previously described (8). The temperature was ramped from room temperature to 800°C at 10°C/min using an LFE temperature programmer. The reactions were carried out in a flow of N_2, CO/N_2, or O_2/N_2 mixture. The catalyst effluent was taken to vent with a small fraction split off normal to the flow path and sent to a Dycor mass spectrometer. This split was passed through a heated, 100-μm capillary about 1 m long before reaching the mass spectrometer. The analysis was done with an electron impact ionization source and a Faraday cup detector. The spectrometer was operated at ca. 10^{-6} Torr using a 70-eV accelerating voltage in the ionizer. Data were collected every 6 sec. The mass spectrometer was calibrated daily to allow conversion of response into micro-moles per unit time. The mass spectrometer, temperature programmer, and mass flow controllers were interfaced with a PC for control and data acquisition.

Variable temperature/controlled atmosphere diffuse reflectance spectra were obtained on a Nicolet 60SX FTIR spectrometer purged with dry nitrogen and equipped with a narrow-band MCT detector. Spectra were acquired at 4 cm^{-1} nominal resolution by coaddition of 256 scans. The diffuse reflectance cell and optics were modified accessories obtained from Harrick Scientific. Sample spectra, consisting of a 10% (w/w) dispersion of sample in predried/ground KCl, were ratioed to the spectrum of pure KCl acquired at the same temperature in all cases. All spectra were acquired in either flowing nitrogen, CO and nitrogen mixtures, or air constantly purging the VT- DRIFT cell.

Subtraction spectra were obtained by taking the difference between the silica support spectrum and the catalyst spectrum (in Kubelka–Munk units) acquired at the same temperature. Subtraction spectra in the OH stretching region were obtained by nulling the 1860-cm^{-1} combination band of silica. Subtraction spectra in the Si–O–M stretching region (1000–750 cm^{-1}) were obtained by nulling the Si–O symmetric stretch of silica gel at 805 cm^{-1}.

RESULTS

Kinetics of $Cr_2(C_2H_3O_2)_7(OH)_2/SiO_2$ Reactions with O_2

To understand the kinetics of the reaction between $Cr_2(C_2H_3O_2)_7(OH)_2/SiO_2$ and oxygen, a series of isothermal studies was done. Water and CO_2 are the only products detected, so decomposition is followed by measuring CO_2 production versus time. Seven runs done at five different temperatures ranging from 271, to 313°C were performed. The data from three, those performed at 271, 293, and 313°C, are plotted as measured rate as a function of conversion in Fig. 1. The fact that the slope of the data is constant versus conversion says two things about the silica supported $Cr_2(C_2H_3O_2)_7(OH)_2$. First, they show that the reactions are first order in the surface species. The generic term "surface species" is used in this case because the data cannot be used to distinguish whether the important component is the entire Cr compound or just an acetate ligand. Second, the strong functional dependence of measured rate on conversion, even to values as high as 80%, indicates that the surface species is distributed homogeneously over the support.

The activation energy for this reaction can be determined in two different ways. The most apparent is to construct an Arrhenius plot using the seven separate isothermal experiments. An alternative method is to apply a kinetic rate law to a temperature-programmed reaction. The CO_2 evolution occurring between 225 and 425°C from such a reaction is represented in Fig. 2. Oxidation occurs in a single event yielding one peak at 333°C. This is more evidence that the surface species is uniformly distributed. The average amount of CO_2 released in 15 separate trials is 824 μmol/g catalyst (Table 1). Assuming that all the carbon

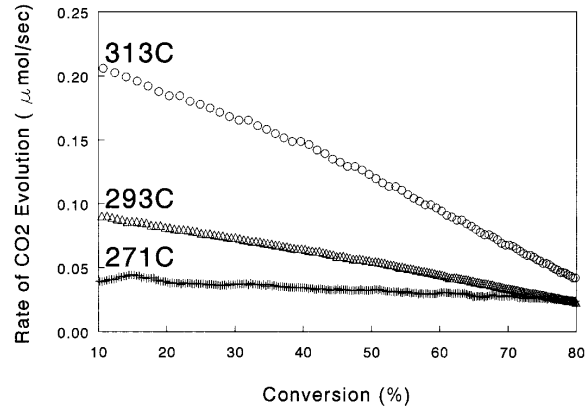

FIG. 1. The rate of CO_2 formation during $Cr_3(C_2H_3O_2)_7(OH)_2/SiO_2$ oxidation versus conversion; the effect of temperature.

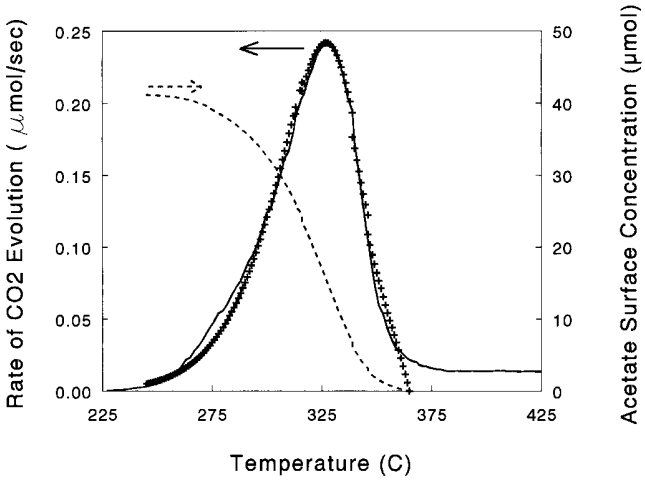

FIG. 2. Mathematical fit of temperature-programmed reaction of $Cr_3(C_2H_3O_2)_7(OH)_3$ in 21% O_2/79% N_2: (—) experimental data, (---) concentration of surface species [S], and (+) mathematical fit (Eq. [1]).

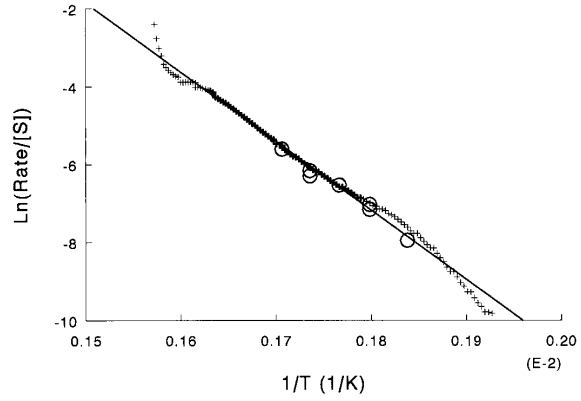

FIG. 3. A comparison of the results from the isothermal experiments (○) with linearized TPRxn data: (+) experimental data; (—) mathematical fit to the linear portion (Eq. [3]).

is from acetate, this would correlate to an acetate/Cr ratio of 2.35 which compares favorably with the expected value of 2.33.

The activation energy can be determined from TPRxn data by first assuming that a simple kinetic power law explains the necessary kinetics:

$$\frac{-d[\mathrm{S}]}{dt} = Ae^{\left(\frac{-E_a}{RT}\right)}[\mathrm{O_2}]^m[\mathrm{S}], \qquad [1]$$

where A is the preexponential factor, E_a is the apparent activation energy, R is the ideal gas constant, T is the reaction temperature, t is the reaction time, $[O_2]$ is the concentration of oxygen, m is the reaction order of oxygen, and [S] is the concentration of surface species.

In a temperature-programmed reaction the temperature is not constant but changes as a function of time, i.e.,

$$T(t) = T_0 + \beta t, \qquad [2]$$

where $T(t)$ is the temperature at time (t), β is the temperature ramp rate, and T_0 is the initial temperature of the experiment.

The analysis can be simplified by choosing conditions such that oxygen is in large excess and unchanging with temperature. This allows its concentration term to be incorporated into the preexponent. The equation is then multiplied by 1/[S]. This concentration term is represented by the dotted line in Fig. 2. Taking the natural log yields a linear equation from which activation energy is easily extracted, i.e.,

$$\ln\left(\frac{1}{[\mathrm{S}]}\frac{-dS}{dt}\right) = \frac{-E_a}{R(T_0 + \beta t)} + \ln(A'), \qquad [3]$$

where $A' = A[\mathrm{O_2}]^m$.

A fit to the linearized TPRxn using Eq. [3] using simple linear regression techniques and the rate data from the isothermal experiments can be compared on the same graph (Fig. 3). This shows that the two methods yield the same information. The value for E_a and A' from these data can be inserted into Eq. [1] to compare the calculation to the experiment. This is represented by the plusses in Fig. 2. An average apparent activation energy of 34.9 kcal/mol with a standard deviation of 2.31 kcal/mol results from the 15 separate TPRxn trials (Table 2). The Arrhenius plot of the

TABLE 1

Quantity of Material Formed during a Temperature-Programmed Reaction of 0.1 g of Silica-Supported $Cr_3(C_2H_3O_2)_7(OH)_2$ in Various Gas Phase Environments

Material and gas phase reagent	CO_2 (μmol/g)		CH_4 (μmol/g)		H_2O[a] (μmol/g)	
	Amount	SD	Amount	SD	Amount	SD
Blank SiO_2 in N_2	ND	—	ND	—	1330	—
$Cr_3(C_2H_3O_2)_7(OH)_2/SiO_2$						
In N_2	480	34.6	264	28.7	798	108
In CO/N_2	1060	80	160	68.5	338	31.6
In O_2/N_2	824	46.1	ND	—	1790	260

[a]Amount reported for water represents chemisorbed water only and does not include physisorbed material.

TABLE 2

The Effects of Gas Flow Rate, Oxygen Concentration and Temperature Ramp Rate on Integrated Peak Areas and Activation Energies Calculated from TPRxn Data

Run No.	Oxygen concentration (%)	Temperature ramp (°C/min)	Flow rate (ml/min)	Integrated peak area (μmol/g-cat)	Apparent activation energy (kcal/mol)
1	21	10	50	796	32.1
2	21	15	50	795	35.0
3	21	15	50	799	39.8
4	21	7	50	756	35.3
5	21	5	50	897	38.0
6	21	5	50	765	35.6
7	21	3	50	799	33.6
8	10.5	10	50	875	36.0
9	10.5	10	50	843	33.0
10	5.2	10	50	844	35.4
11	5.2	10	50	855	36.9
12	15.8	10	50	823	33.8
13	21	10	100	858	31.2
14	21	10	50	888	32.4
15	21	10	50	762	35.9

seven isothermal runs alone gives an activation energy of 33.0 kcal/mol which is within a single standard deviation of the TPRxn mean.

The reaction order of oxygen can now be addressed. Kinetic studies have traditionally been done by varying reagent concentration at a constant temperature. It has also been demonstrated that a series of TPRxns employing different gaseous reagent concentrations may be used (9). The benefit of the latter is the larger amount of information available from the temperature-programmed methods. In the current study a series of TPRxns were run with oxygen compositions ranging from 0.5 to 21%. It can be seen that as the gas mixture becomes more oxygen rich, the combustion peak shifts to a lower temperature (Fig. 4). A temperature is chosen where all the peaks overlap, and the extent of reaction at any one composition never exceeds 25%. These criteria are met at 303°C. The amplitude of the response at any particular temperature represents rate data. The data from both TPRxn and isothermal studies over similar oxygen compositions are plotted in ln(rate) vs ln[O_2] format in Fig. 5. A single line with a slope of 0.44 can be fit to the combined data set. The correlation coefficient of 0.96 indicates that the two procedures generate the same information.

The set of results from this study can be combined into a proposed rate expression for the activation of silica supported basic chromium acetate in oxygen:

$$-\frac{d[\mathrm{OAc}]}{dt} = k[\mathrm{OAc}]\,[\mathrm{O_2}]^{0.44}.$$

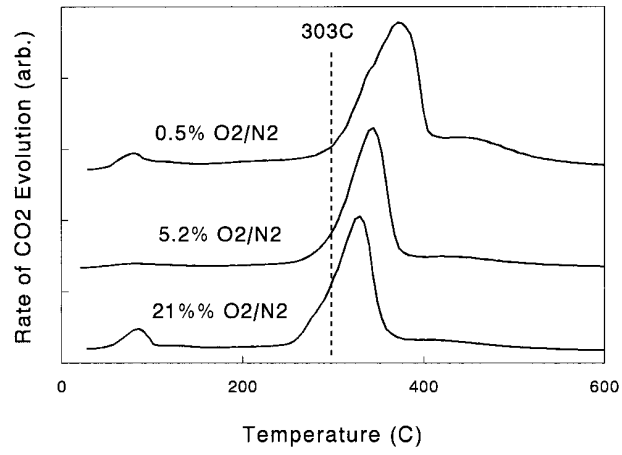

FIG. 4. The effect of oxygen partial pressure on the TPRxn of $Cr_2(C_2H_3O_2)_7(OH)_2$.

Decomposition of $Cr_2(C_2H_3O_2)_7(OH)_2/SiO_2$ in N_2 and CO

The close agreement between isothermal and TPRxn techniques shows that they can be interchanged as necessary. This is helpful in cases where isothermal experiments become difficult as is true for the autodecomposition of $Cr_3(C_2H_3O_2)_7(OH)_2/SiO_2$ in N_2. The primary TPRxn products of this reaction are CO_2 ($m/e = 44$), CH_4 ($m/e = 15$, from methyl), and H_2O ($m/e = 18$) (Fig. 6). Surprisingly, no acetic acid ($m/e = 60$) is detected. Acetate decomposition begins at ca. 350°C and reaches a rate maximum at ca. 425°C. Evolution of carbon continues (as CO_2 and CH_4) past 500°C and reaches baseline levels by 800°C. The quantities of material formed in this and the other TPRxns are presented in Table 1. The average amount of CO_2 generated in five trials is 480 μmol/g catalyst (SD = 34.6 μmol/g).

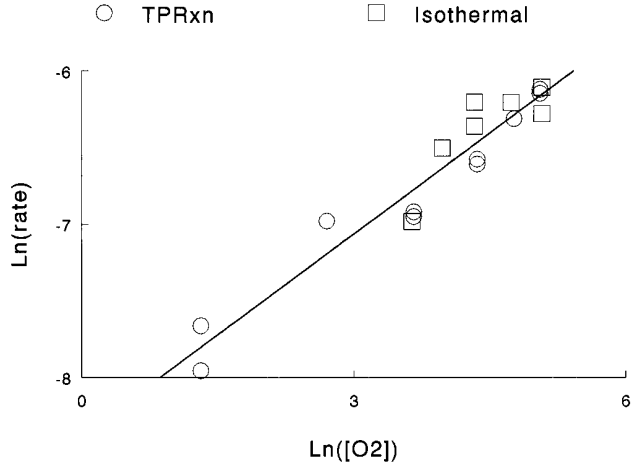

FIG. 5. Plot of ln(rate) versus ln[O_2] from isothermal and TPRxn studies. The rate data were collected at 303°C.

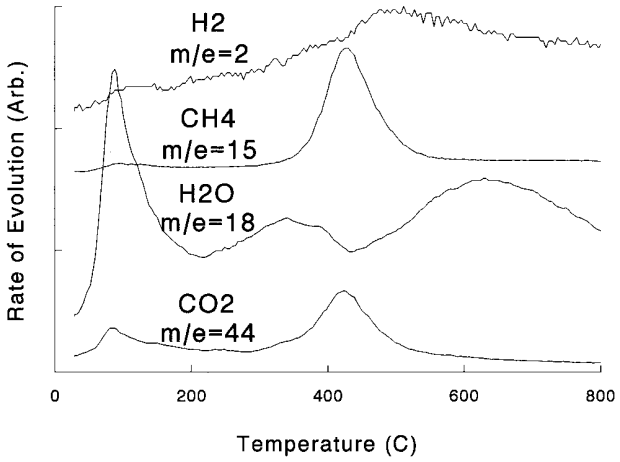

FIG. 6. Temperature-programmed reaction of $Cr_3(C_2H_3O_2)_7(OH)_3/SiO_2$ in N_2.

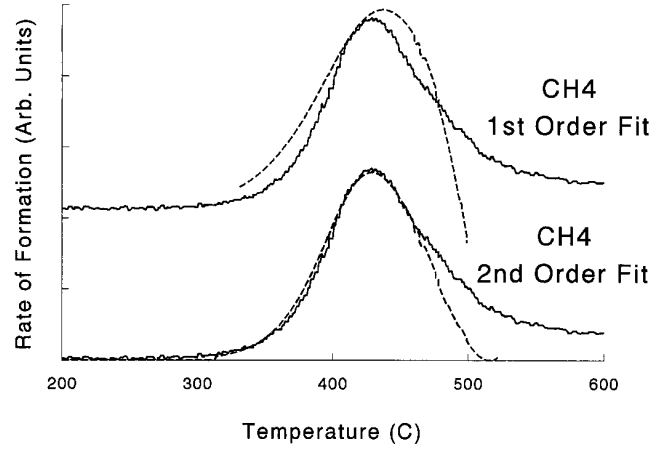

FIG. 8. Methane formation data generated in $Cr_3(C_2H_3O_2)_7(OH)_3/SiO_2$ TPRxns under N_2 as it is fit with kinetic models assuming first- and second- order dependence upon acetate: (—) experimental data, (- - -) mathematical fits.

Average methane is 264 μmol/g (SD = 28.7 μmol/g). These two constituents account for just over 85% of the carbon initially present. The remaining carbon is retained by the surface under nitrogen, but can be removed by oxidation. Water formed from silanol condensation during decomposition averages 798 μmol/g (SD = 108 μmol/g). The water profile will be discussed separately when the role of surface hydroxyl groups is addressed. Some hydrogen ($m/e = 2$) formation is also detected during decomposition but the precise amount is difficult to quantify.

The temperature-programmed reaction done in CO/N_2 mixtures is very similar to that in N_2 (Fig. 7). Again, CO_2, CH_4, H_2O, and H_2 are formed. The shape of the profiles differ somewhat, and the quantities released are different (Table 1).

The methane profile from the decomposition in N_2 is fit with a kinetic rate law in Fig. 8. For current purposes, we are only interested in the initial stages of decomposition so only the low temperature peak (<520°C) is fit. Approximating the reaction order of the surface species as one yields a poor fit, whereas a second-order approximation fits the data very well (Fig. 8). The fit sum of squares error between 315 and 460°C is 8.3% of the area for first order; it drops to 0.7% for second-order. The initial generation of CO_2 in N_2 can also be modeled assuming second-order kinetics. These fits yield activation energies of 36.2 and 34.4 kcal/mol for CH_4 and CO_2 formation, respectively. Averaging the results from 10 experiments (Table 3) generates an activation energy of 36.5 kcal/mol (SD = 2.2 kcal/mol) for CH_4 formation and 33.9 kcal/mol (SD = 4.2 kcal/mol) for CO_2 formation. Inspection of Table 3 shows that in 8 of the 10 trials the activation energy for CO_2 formation is lower than that of CH_4. A paired t test reveals that the two means are indeed different to a 95% level of confidence.

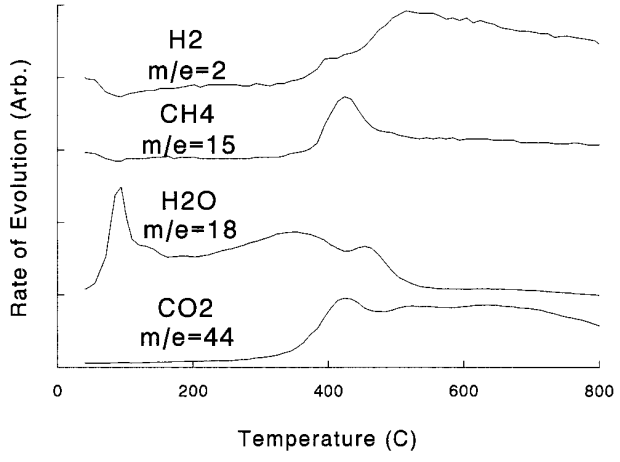

FIG. 7. Temperature-programmed reaction of $Cr_3(C_2H_3O_2)_7(OH)_3/SiO_2$ in 10% CO in N_2.

When the decomposition is done in CO/N_2 mixtures, the CO_2 profile is difficult to fit due to the large number of convoluted peaks (Fig. 7). However, the CH_4 profiles can be fit, assuming a surface species kinetic order of 2. The resulting average activation energy from seven trials (Table 3) is 38.0 kcal/mol (SD = 3.8 kcal/mol). A standard t test comparing this with that obtained from fitting the methane data collected in N_2 (vide supra) reveals that these means are not significantly different at the 95% level of confidence. The agreement between these two distributions suggests that the same transition state is occurring in both environments.

The activation energy values in N_2 and CO/N_2 mixtures are comparable to the average of 34.9 kcal/mol (SD = 2.31 kcal/mol) obtained when done in oxygen mixtures. A comparison of CO_2 evolution in the three different atmospheres shows that oxygen causes a 90°C drop in the CO_2 peak maximum (Fig. 9). This may be related to the kinetics operating

TABLE 3

Calculated Activation Energies from Temperature-Programmed Reaction of Silica-Supported $Cr_3(C_2H_3O_2)_7(OH)_2$ in CO and CO/N_2 Mixtures

Trial	CO concentration (%)	CO_2 activation energy (kcal/mol)	CH_4 activation energy (kcal/mol)
1	0	29.7	35.7
2	0	31.4	36.1
3	0	37.0	38.6
4	0	33.3	36.8
5	0	39.8	36.1
6	0	34.4	36.2
7	0	27.4	33.5
8	0	30.3	32.2
9	0	39.0	38.2
10	0	36.6	40.4
11	3	—	33.1
12	5	—	33.6
13	10	—	39.6
14	10	—	44.1
15	15	—	38.7
16	20	—	38.1
17	20	—	38.4

in the respective systems. In N_2 the reaction order of the surface species is ca. 2, while in oxygen the reaction is first order in acetate and 1/2 order in O_2. This will be discussed more fully below.

Role of Hydroxyl Groups

As discussed in the Introduction, it has been observed that the silica hydroxyl population influences final catalyst behavior (1–3). Comparing the various TPRxns shows that

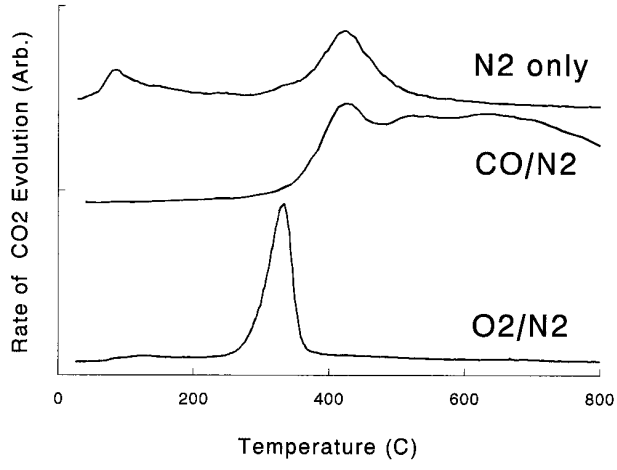

FIG. 9. CO_2 formation during $Cr_3(C_2H_3O_2)_7(OH)_3/SiO_2$ TPRxns in inert, reducing, and oxidizing environments.

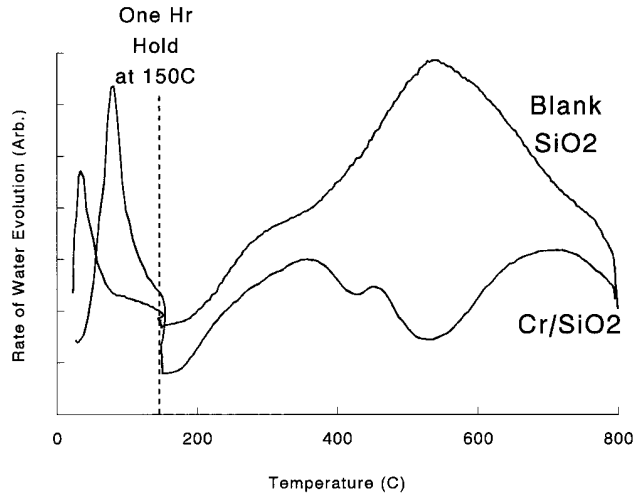

FIG. 10. Comparison of H_2O formation from blank SiO_2 with $Cr_3(C_2H_3O_2)_7(OH)_3/SiO_2$ TPRxns in N_2.

the Cr compound influences the dehydroxylation of SiO_2. In contrast, when Cr is absent from the support, the dehydroxylation of SiO_2 appears the same independent of whether the reagent gas is oxidizing, reducing, or inert. Figure 10 contains the H_2O profiles from dehydroxylation in N_2 of bare SiO_2 and SiO_2 supported basic chromium acetate. In order to reduce the amount of error introduced into the analysis by physisorbed water the samples were held at 150°C for 1 h prior to resuming the temperature ramp. These data show that the amount of hydroxyls removed from the support as water is decreased in the presence of Cr by 40% (Table 1). Over bare SiO_2, a broad set of water peaks appear centered at 540°C. When Cr is present, two, apparently separate, processes occur. The first exhibits a peak maximum at 350°C and a shoulder at ca. 450°C. The maximum rate of the second occurs at 710°C. This profile resembles that of bare SiO_2 with the exception of a peak attenuation occurring between 400 and 600°C (Fig. 10). This is the temperature range where $Cr_3(C_2H_3O_2)_7(OH)_2/SiO_2$ decomposes (Fig. 6). Table 1 also shows that the oxygen present in the CO_2 produced during decomposition in N_2 is greater (960 μmol O/g) than the amount expected from acetate alone (816 μmol O/g based on Cr loading). The extra oxygen may be coming from the surface.

Interaction of the Cr compound and the surface during decomposition and dehydroxylation can be further shown with CO as the reagent. Figure 11 compares the H_2O profiles from the TPRxns of $Cr_3(C_2H_3O_2)_7(OH)_2/SiO_2$ in each of the three different atmospheres, i.e., oxidizing, inert, and reducing. The three traces are quite different. In oxygen, water is formed in two processes. The first is the combustion of acetate groups with a rate maximum at 340°C. The second appears to be the condensation of surface silanols centered at 545°C. The water evolution in N_2 has already been discussed. The same low-temperature process appears

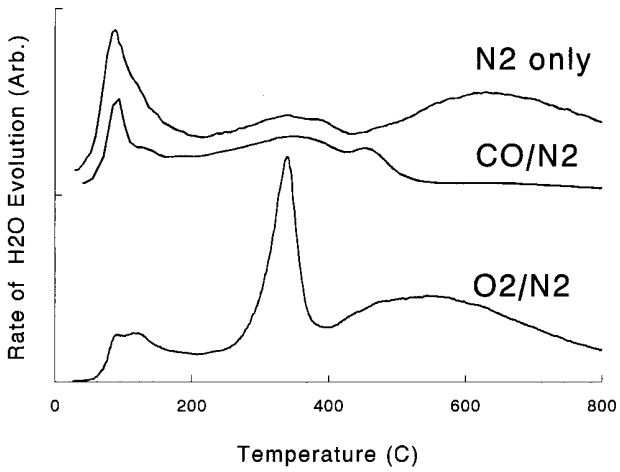

FIG. 11. H_2O formation during $Cr_3(C_2H_3O_2)_7(OH)_3/SiO_2$ TPRxns in inert, reducing, and oxidizing environments.

in CO as it does in N_2. However, at temperatures greater than 500°C water formation is suppressed. Integration of the respective profiles show that more than twice the water is released in N_2 relative to CO/N_2 (Table 1).

The differences between the water profiles can be explained with the help of the CO_2 profiles from the TPRxns done in each of the three atmospheres (Fig. 9). In 21% O_2 decomposition occurs quickly and is virtually finished at temperatures where it only begins in the other two media. Yet, even though CO_2 production in these two media initially appears similar and show maxima at 425°C, at temperatures above this they are quite different. The amount of CO_2 produced in CO is greater (1060 μmol/g) than that formed in either inert or oxidizing systems (Table 1). Unlike the effect of increasing O_2 partial pressure (Fig. 4), the position of the CO_2 peaks is not influenced by changes in CO partial pressure. Therefore, the decomposition appears to be zero order in CO.

The differences in CO_2 and H_2O profiles can be explained by reactions of silica silanol groups analogous to the water gas shift as previously proposed (4, 6), i.e.,

$$\begin{matrix} OH & OH & & & & O & \\ | & | & & & & / & \backslash \\ Si & Si & + CO \dashrightarrow & CO_2 + H_2 + & Si & & Si \end{matrix}$$

This explanation is further supported by a, qualitatively, greater H_2 yield in CO relative to N_2. Although H_2 evolution is difficult to quantify, visual inspection of the H_2 profiles in Figs. 6 and 7 indicates a difference. For the water gas shift reaction to occur at these temperatures Cr must interact with the surface and be involved in the catalysis.

Variable-Temperature Diffuse-Reflectance Infrared

Variable-temperature diffuse-reflectance infrared studies also reveal an intimate association between $Cr_3(C_2H_3O_2)_7(OH)_2$ and SiO_2 hydroxyls. The changes in catalyst surface structure in an oxidizing atmosphere are presented in Fig. 12 (OH stretching region) and 13 (Cr=O, Si–O region). Each spectrum is recorded as the difference between $Cr_3(C_2H_3O_2)_7(OH)_2/SiO_2$ and blank support at the temperature listed. An inverse band indicates a loss of absorbance induced by the chromium species, whereas a positive peak indicates absorbance related to these groups. Therefore, the inverse peak at ca. 3740 cm^{-1} in Fig. 12 indicates a loss of non-hydrogen-bonded silanols. This loss may be due to a chemical reaction that consumes the silanols, or a physical interaction with the chromium species that changes the band position. The latter would cause a band shift and, thus, be accompanied by a positive peak at a different frequency. Consumption of silanols would result in an inverted peak only. A broad peak at <3600 cm^{-1} in the OH stretching region (Fig. 12) indicates a shift in absorbance due to physical interactions. This peak is present at low temperatures and shrinks significantly by 300°C. By 400°C no positive absorbance is detected, and the strong negative peak at 3740 cm^{-1} remains. The high-temperature spectrum agrees with data previously reported (10). It suggests that physisorption of the Cr compound occurs initially to shift the OH stretching band of non-hydrogen-bonded silanol groups. The high-temperature calcination

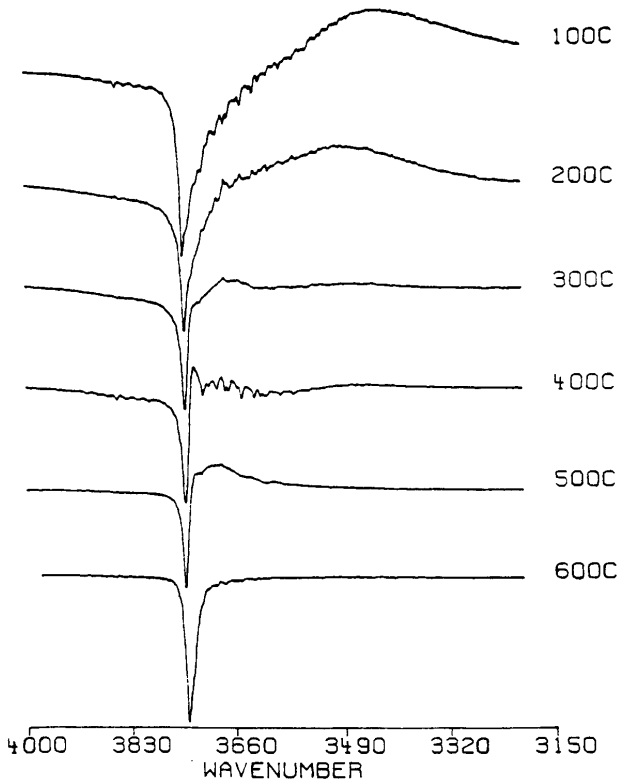

FIG. 12. VT-DRIFT spectra of the O–H stretching region during the reaction of $Cr_3(C_2H_3O_2)_7(OH)_3/SiO_2$ in 21% O_2/N_2.

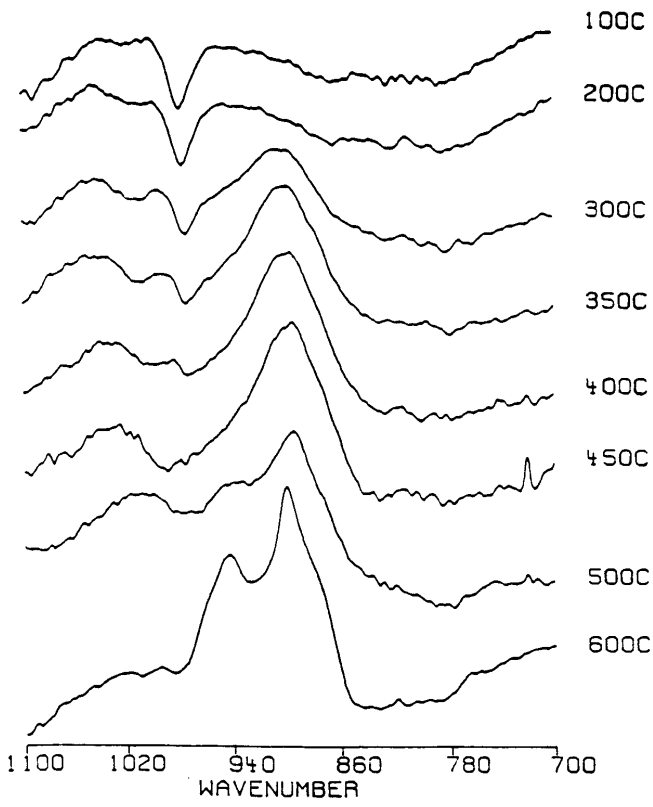

FIG. 13. VT-DRIFT spectra of the Cr–O stretching region during the reaction of $Cr_3(C_2H_3O_2)_7(OH)_3/SiO_2$ in 21% O_2/N_2.

in air which follows causes chemisorption to occur which *consumes* these silanols between 200 and 400°C. This temperature range coincides with TPRxn recorded decomposition of the Cr compound.

Subtraction spectra of air decomposed basic chromium acetate in the lower frequency region are shown in Fig. 13. No detectable absorbance is seen at 200°C or less, but at 300°C a band is detected at 900 cm^{-1}, which has been assigned to a Cr=O stretch (11, 12). This assignment supports our determination of 1/2 order O_2 kinetics, since oxygen appears to be dissociatively activated by Cr. At 400°C the 900-cm^{-1} band dominates the subtraction spectrum, but at 500–600°C a new band is detected at 945 cm^{-1}. We are not aware of any assignment of this band, though both absorbances have been observed previously (11). It appears that the 945-cm^{-1} band, like that at 900 cm^{-1}, is due to Cr–O bonds differing from those in $Cr_3(C_2H_3O_2)_7(OH)_2$. Two possible explanations come to mind. The first is that the two bands represent symmetric and asymmetric stretches of the O=Cr=O group. This would necessitate that both would become visible only after complete destruction of the Cr precursor which establishes the proper symmetry. On the other hand it may represent a stretch in the Si–O–Cr group.

Very little difference is observed in the VT-DRIFT analyses done in N_2 and CO/N_2 mixtures. Therefore, only those done in N_2 are shown in Figs. 14 and 15. The corresponding subtraction spectra in the OH stretching region show a inverted peak at approximately 3740 cm^{-1} (Fig. 14). As with the subtraction spectra in air, the loss is initially accompanied by a positive peak at a lower frequency indicating a band shift. Unlike the air spectra, however, this shift persists at higher temperatures and finally results in a sharp, positive peak at 3733 cm^{-1} by 600°C. So, although the losses of acetate and isolated silanols are concerted in air, in N_2 the silanols are preserved and hydrogen bonded with the Cr species throughout the decomposition. With hydrogen bonding as the only detected interaction between the Cr species and the support, it would follow that Cr is fairly mobile at these high temperatures. This is supported by previous observations (6) and models proposed (12) to explain these systems.

The low frequency end of the IR shows no evidence of Si–O–Cr or Cr=O bond formation (Fig. 15). The Si–O stretch of Si–O–Cr species is expected in the 975- to 875-cm^{-1} region. Results of spectral subtraction do not reveal any detectable absorbance. These data along with the spectra shown in Fig. 13 suggest that little or no Cr–O–Si bond formation occurs in nitrogen in this temperature range.

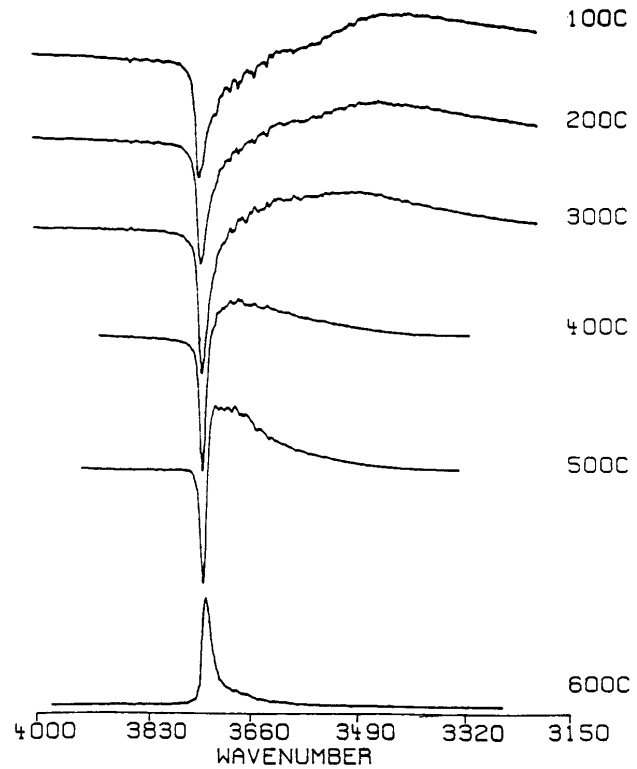

FIG. 14. VT-DRIFT spectra of the O–H stretching region during the reaction of $Cr_3(C_2H_3O_2)_7(OH)_3/SiO_2$ in N_2.

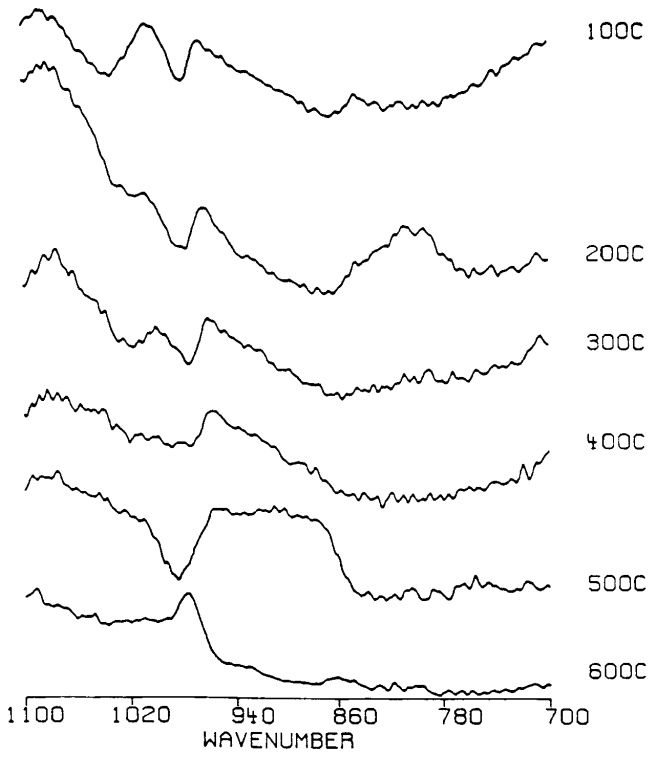

FIG. 15. VT-DRIFT spectra of the Cr–O stretching region during the reaction of $Cr_3(C_2H_3O_2)_7(OH)_3/SiO_2$ in N_2.

DISCUSSION

A Mechanism for $Cr_3(C_2H_3O_2)_7(OH)_2/SiO_2$ Activation

The initial morphology of $Cr_3(C_2H_3O_2)_7(OH)_2$ on SiO_2 is difficult to know with certainty, but it may be inferred by the data. First, isothermal and TPRxn studies show that the decompositions are very uniform. This would suggest that the environment surrounding each basic chromium acetate domain is very similar. Second, the TPRxns also show that there is extensive interaction between the support and the Cr compound. VT-DRIFTS confirms this by showing a significant perturbation in the SiO_2 hydroxyl stretching frequency when $Cr_3(C_2H_3O_2)_7(OH)_2$ is present. The third factor to consider is the capacity of the support. It is generally accepted that there are 4.5 hydroxyl groups per square nanometer of silica surface (13). Using this number one can calculate that at the Cr loading of our material there are 12.8 surface silanols per Cr. These three observations would indicate that, upon deposition, the Cr precursor forms two-dimensional islands on the SiO_2 support.

The critical next step in the activation of a Cr/SiO_2 catalyst appears to be destruction of the ligand shell surrounding the Cr atom. Evidence from TPRxns suggests that this begins at the methyl group of the acetate. In O_2/N_2 mixtures the reaction is 1/2 order in oxygen suggesting that dissociation occurs prior to the rate limiting step. If decomposition were to begin at the carboxylate group, then only rearrangement to CO_2 and no addition of oxygen would be necessary. However, conversion of methyl to CO_2 and H_2O is accelerated by oxygen activation. In this scenario Cr, known to be a good combustion catalyst (14), serves as the active site for the destruction of its own ligand shell. The single CO_2 peak in the O_2/N_2 profile in Fig. 9 indicates that rearrangement of the carboxylate moeity to gaseous CO_2 and combustion of the methyl group occur simultaneously.

Further support for methyl loss as the rate-limiting step in acetate decomposition can be gathered from the studies in N_2. In this case CO_2 production is concurrent with CH_4 even though it possesses a measurably lower activation energy. A mechanism such as this can explain several observations. The first is the 90°C difference in CO_2 and CH_4 formation in N_2 and CO/N_2 mixtures relative to oxidizing environments. If decomposition is limited by methyl group loss then each acetate must find another acetate in order to abstract a hydrogen prior to releasing CH_4. This requires temperatures high enough to induce migration of the Cr compound on the surface. This also explains the second-order kinetics of the surface species in nonoxidizing environments. The VT-DRIFTS experiments also suggest that migration can occur. No apparent chemical bonds with the surface are formed in inert or reducing atmospheres, yet the spectra suggest that hydrogen bonding does occur, as previously proposed (12). Evidence has been shown that surface Cr species do migrate and agglomerate at high temperatures (6). Finally, since a methyl group may yield several hydrogen atoms to departing methane molecules, a small fraction of the carbon should be retained in an inert environment. We measure this amount to be ca. 15% of that initially present.

The data in this report also show an interaction between the Cr compound and the surface hydroxyls during decomposition and dehydroxylation. Simply depositing basic chromium acetate onto silica alters the way the support dehydroxylates (Fig. 10). The decrease in the number of hydroxyl groups leaving the surface as water may be explained in a couple of ways. The first is that the Cr compound displaces hydroxyl groups upon deposition; however, evidence from VT-DRIFTS does not support this. According to these data, hydroxyl groups are not removed; their stretching frequency is only perturbed (Fig. 14). A better explanation is that the Cr/SiO_2 association is so intimate that upon decomposition hydroxyls groups surrounding the compound react with the ligands. This would account for the amount of CO_2 evolved being larger than expected during decomposition in N_2 (Table 1). It would also explain why the attenuation in the water profile coincides with decomposition of the Cr compound (Fig. 10). When the decomposition occurs in CO, Cr appears to be free to catalyze a water–gas shift reaction to catalytically remove surface hydroxyl groups. In oxygen, VT-DRIFTS and TPRxn data together suggest

that chromium oxygen bonds form concomitantly with, and subsequent to, ligand shell destruction. In every case, it appears clear that the presence of Cr does increase the extent of surface dehydroxylation, as previously proposed (4–6).

CONCLUSIONS

Both TPRxn and VT-DRIFTS studies confirm that while the decomposition of basic chromium acetate is similar in inert (N_2) and reducing (CO/N_2) environments, the activation process is fundamentally different in an oxidizing (O_2/N_2) environment. In inert and reducing environments the major decomposition products are CH_4 and CO_2. In oxidizing atmosphere, the major products are CO_2 and H_2O. The kinetics also differ. In inert and reducing environments the decomposition is second order with respect to the surface species, whereas in oxygen it is first order with respect to acetate and 0.5 order with respect to oxygen.

The data also reveal an intimate association between the basic chromium acetate molecule and local silica hydroxyls. In each of the three media studied, the presence of Cr influences the dehydroxylation of the support. In N_2, hydroxyl groups appear to react with decomposing acetate ligands increasing the amount of CO_2 formed from the reaction. In CO, Cr appears to catalyze a water–gas shift reaction producing CO_2 and H_2 from CO and surface hydroxyl groups. VT-DRIFTS shows no evidence of Cr–O–Si bond formation in these two media. However, loss of silanols in oxidizing environments suggests surface bond formation in the 200–400°C range.

The apparent lack of surface bond formation in inert and reducing atmospheres suggests that at higher temperatures Cr species can migrate about the surface. This can explain the second-order decomposition kinetics with respect to acetate, since two acetates must come into contact to produce CH_4. In all cases the rate-limiting step is removal of the acetate methyl group.

Since HDPE catalysts based on silica-supported chromium are so sensitive to activation conditions, this information is a step toward understanding the underlying chemistry behind the observed differences.

ACKNOWLEDGMENT

The authors thank Michael P. Benson, Ph.D., for many helpful and challenging discussions regarding this paper.

REFERENCES

1. "Monthly Petrochemical and Plastics Analysis," p. 45. Chemical Data, June 1994.
2. McDaniel, M. P., *Adv. Catal.* **33**, 47 (1985).
3. Myers, D. L., and Lunsford, J. H., *J. Catal.* **92**, 260 (1985).
4. Jozwiak, W. K., Dalla Lana, I. G., and Fiedorow, R., *J. Catal.* **121**, 183 (1990).
5. McDaniel, M. P., and Welch, M. B., *J. Catal.* **82**, 98 (1983).
6. McDaniel, M. P., *J. Catal.* **67**, 71 (1981).
7. Welch, M. B., and McDaniel, M. P., *J. Catal.* **82**, 110 (1983).
8. Augustine, S. M., and Blitz, J. P., *J. Catal.* **142**, 312 (1993).
9. Groeneveld, C., Witgen, P. P. M. M., van Kersbergen, A. M., Mestrom, P. L. M., Nuijten, C. E., and Schuit, G. C. A., *J. Catal.* **59**, 153 (1979).
10. Nishimura, M., and Thomas, J. M., *Catal. Lett.* **21**, 149 (1993).
11. Kim, C. S., and Woo, S. I., *J. Mol. Catal.* **73**, 249 (1992).
12. Zecchina, A., Garrone, E., Ghiotti, G., Morterra, C., and Borello, E., *J. Phys. Chem.* **79**, 966 (1975).
13. Zhuravlev, L. T., *Coll. Surf. A,* **74**, 71 (1993).
14. Hill, W., and Ohlmann, G., *J. Catal.* **123**, 147 (1990).